

# Monomer-to-Water Ratios as a Tool in Controlling Emulsion Copolymer Composition: The Methyl Acrylate–Indene System

LILIAN F. J. NOËL, JAN M. A. M. VAN ZON, and ANTON L. GERMAN\*

Department of Polymer Chemistry and Technology, Eindhoven University of Technology, 5600 MB Eindhoven, The Netherlands

## SYNOPSIS

A drifting copolymer composition as a function of conversion is an aspect typical of copolymerization. Reducing this so-called composition drift in batch copolymerizations will lead to a decrease in chemical heterogeneity of the copolymers formed. For monomer systems in which the more water-soluble monomer is also the more reactive one, theory predicts that composition drift in emulsion copolymerization can be reduced or even minimized by optimizing the monomer-to-water ratio. The monomer combination methyl acrylate–indene (MA–Ind) meets the requirements needed to minimize composition drift in batch emulsion copolymerization. Therefore, this monomer combination is chosen as a model monomer system in order to verify this theoretical prediction. Reactivity ratios needed for model predictions have been determined by low conversion bulk polymerization, resulting in  $r_{MA} = 0.92 \pm 0.16$  and  $r_{Ind} = 0.086 \pm 0.025$ . Furthermore, emulsion copolymerization reactions at the same monomer mole fraction are performed at different monomer to water ratios. From the good agreement between experiments and theoretical predictions for MA–Ind, it was concluded that control and even minimization of composition drift in batch emulsion copolymerization for monomer systems in which the more water-soluble monomer is also the more reactive one is indeed possible by changing the initial monomer-to-water ratio of the reaction mixture provided that the reactivity ratios of both monomers are not too far from unity. © 1994 John Wiley & Sons, Inc.

## INTRODUCTION

Composition drift occurring in *ab initio* batch emulsion copolymerization will lead to chemically heterogeneous copolymers. To control composition drift, semicontinuous emulsion copolymerization processes have been developed. The various addition strategies used in semicontinuous processes include (1) the addition of a given monomer mixture at a constant rate lower than the polymerization rate (starved conditions)<sup>1–9</sup> and (2) the addition of monomer(s) at an optimal addition profile with addition rates higher than the polymerization rate (flooded conditions).<sup>10–14</sup> Disadvantages of these

strategies are the relatively long reaction times, especially under starved conditions, and the time-consuming determination of the optimal addition profile, which, furthermore, requires an immediate start of reaction since inhibition hampers the addition procedure. For monomer systems in which at least one of the monomers has a relatively high but limited water solubility, a different approach can be used to influence composition drift. When a monomer has a relatively high but still limited water solubility, a certain amount of that monomer will be located in the aqueous phase, thus influencing the monomer ratio and concentrations within the polymer particle phase. Since this polymer particle phase is considered to be the main locus of reaction, the monomer ratio and monomer concentrations within the polymer phase control both copolymer composition and polymerization rate. Depending on the

\* To whom correspondence should be addressed.

amount of water in the reaction mixture, i.e., depending on the monomer-to-water ratio (M/W), more or less monomer will be dissolved in the aqueous phase. It should be noted that efforts to raise the final solid content of a latex will change the monomer-to-water ratio and thus, in many cases, the copolymer composition of the product. By adding more water to the reaction mixture, the more water-soluble monomer can be withdrawn from the particles and thus from reaction. If the monomer with the higher water-solubility is also the less reactive one, composition drift can be enhanced by decreasing the monomer-to-water ratio. A system that illustrates this is the system methyl acrylate-indene.<sup>15</sup> In principle, it should be possible to lower or even minimize composition drift for monomer combinations where the more water-soluble monomer also is the more reactive one. Since the water-solubilities of the monomers methyl acrylate (MA) and indene (Ind) differ by two orders of magnitude and since MA is not only the more water soluble but also the more reactive monomer, the somewhat unusual monomer combination MA-Ind is chosen as an example to show that minimization of composition drift is indeed possible just by changing monomer-to-water ratios. The structural formula of indene (C<sub>9</sub>H<sub>8</sub>) is shown in Figure 1. Note that although the monomer system MA-Ind is an ideal monomer combination to verify theoretical predictions other monomer combinations in which the more water soluble monomer is also the more reactive one also comply with the theory. However, it is important to realize that for reactivity ratios that are far apart composition drift can only be minimized if the water-solubility of the monomers is also very far apart. Otherwise, unrealistic and impractical monomer-to-water ratios will be required or, in extreme situations, minimum composition drift *cannot* be achieved in batch emulsion copolymerization by simply changing the monomer-to-water ratio.

In this article, effects of increasing both the initiator and surfactant concentrations upon the MA-Ind conversion-time curves are discussed and the

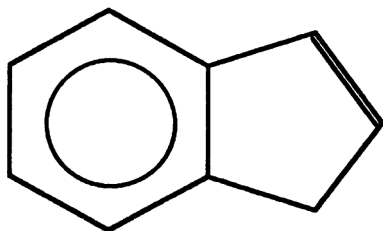


Figure 1 Structural formula of the monomer indene.

reactivity ratios of the monomer system MA-Ind are determined from low-conversion bulk polymerization. On this basis, emulsion copolymerization reactions are performed with similar initial overall monomer mole feed ratios and with changing monomer-to-water ratios.

Based on simplifications of generally accepted thermodynamic relationships,<sup>16-20</sup> more accessible theories have been developed<sup>21,22</sup> to describe monomer partitioning for latex particles with two monomers. Combining these relationships for monomer partitioning with mass balances enables one to predict emulsion copolymerization in terms of composition drift and absolute concentrations of monomers in the particle and aqueous phase<sup>23</sup> as a function of conversion. Effects of different monomer-to-water ratios and the use of a seed polymer in emulsion copolymerizations on the course of reaction in terms of composition drift can be predicted very well.<sup>23</sup> Composition drift is minimized for the monomer combination MA-Ind and experimental results of *ab initio* batch emulsion copolymerizations are compared with model predictions.

## THEORY

The copolymerization equation relates the instantaneous copolymer composition with the reactivity ratios and monomer feed composition for solution and bulk polymerizations<sup>24,25</sup>:

$$F_i = \frac{r_i \cdot f_{pi}^2 + f_{pj} \cdot f_{pi}}{r_i \cdot f_{pi}^2 + 2 \cdot f_{pi} \cdot f_{pj} + r_j \cdot f_{pj}^2} \quad (1)$$

where  $F_i$  stands for the copolymer composition in mole fraction of monomer  $i$ ;  $f_{oi}$  and  $f_{oj}$  are the overall monomer mole fractions in the polymer phase of monomers  $i$  and  $j$ ; and  $r_i$  and  $r_j$ , the reactivity ratios of monomers  $i$  and  $j$  in the selected monomer combination  $i-j$ . In solution and bulk copolymerization of the monomer system  $i-j$  with reactivity ratios lower than unity, conditions can be reached where the monomer mole fraction equals the copolymer composition of the instantaneously formed copolymer ( $f_i = F_i$ ). At these so-called azeotropic conditions, there will be no composition drift, i.e., the instantaneous copolymer composition remains constant during conversion.

If there is a separate aqueous phase present as in emulsion copolymerization, the simple theory predicting azeotropic conditions becomes complicated. For monomers with relatively high, but still limited

water solubility, a considerable amount of the monomer can be dissolved in the aqueous phase. Since polymerization is assumed to occur in the polymer particles, the amount of monomer dissolved in the aqueous phase will affect the monomer mole fractions in the particle phase. In these emulsion copolymerizations, the copolymerization equation [eq. (1)] can still be used, but instead of the overall monomer mole fraction,  $f_{oi}$ , the monomer mole fraction in the polymer phase,  $f_{pi}$ , should be used. For monomer combinations in which at least one of the monomers has a relatively high, but still limited water solubility, composition drift will occur with increasing conversion, even if conditions are chosen in which the prerequisite for azeotropic conditions, i.e., instantaneous copolymer composition equals the overall monomer mole composition, is met. The reason that azeotropic conditions cannot be maintained over a wide range of conversion in emulsion copolymerization is caused by the effect of changing monomer-to-water ratios and increasing polymer volumes on the monomer mole fraction in the polymer particles as conversion increases. In emulsion copolymerizations, where at least one of the monomers in the selected monomer combination has a relatively high, but limited water solubility, composition drift cannot be avoided; it can only be minimized. Theoretically, this minimum composition drift can be obtained for several overall monomer mole fractions by using the heterogeneity of the emulsion system. This is in contrast with solution or bulk polymerization, where azeotropic conditions can only be obtained at one overall monomer mole fraction. Exact azeotropic behavior in emulsion copolymerization can be obtained only in the following cases: (1) if both monomers in the chosen monomer combination have low water solubility, leading to negligible amounts of monomer in the aqueous phase as compared to the amount of monomers in the organic (monomer droplet and polymer particle) phase, or (2) if the ratio of the water solubilities is equal to unity, leading to identical monomer mole ratios in the aqueous phase and in the polymer phase. Note that in the above cases changing the monomer-to-water ratios has no effect on the course of emulsion polymerization.

As stated above, theoretically, it should be possible to control and minimize composition drift for monomer combinations where the more water-soluble monomer also is the more reactive one. Based on the water solubility of the monomers, an amount of monomer is withdrawn from the monomer droplets and polymer particles, thus affecting the monomer ratio within the polymer phase and therefore

having an effect on the copolymer formed. If monomer  $i$  is chosen to be the monomer with the highest water solubility, the mole fraction of monomer  $i$  in the copolymer will reach a maximum value when all the monomer is located in the polymer particle and monomer droplet phase (comparable with solution and bulk polymerizations), and it will reach a minimum value when all the monomer is located in the aqueous phase. The value for the minimum mole fraction of monomer  $i$  strongly depends upon the ratio of the water solubility of monomer  $j$  over the water solubility of monomer  $i$ , from here on denoted as the  $\alpha$ -value. It has been reported<sup>23</sup> that the difference between maximum and minimum monomer mole fractions will be the largest for small  $\alpha$ -values. In such cases, changing the monomer-to-water ratio or polymer volume will have the strongest effect upon the monomer mole fraction in the polymer phase. It is in these cases that, for monomer systems in which the more reactive monomer is also the more water-soluble one, minimum composition drift can be obtained by changing the monomer-to-water ratio.

## EXPERIMENTAL

### Materials

The following materials were used for emulsion copolymerization reactions: reagent-grade methyl acrylate (MA, Janssen Chimica, Tilburg, The Netherlands) and indene, tech., 90+% (Ind, Janssen Chimica), doubly distilled water, sodium persulfate (p.a., Fluka AG, Buchs, Switzerland) as the initiator, sodium dodecyl sulfate (SDS, Fluka), and anterox CO-990 (Ant CO-990, GAF, Delft, The Netherlands) as surfactant and sodium carbonate (p.a., Merck, Darmstadt, Germany) as the buffer. Before use, the MA was distilled under reduced pressure to remove the inhibitor. The middle fraction was cut and stored at 4°C. The indene was purified by shaking 0.5 L indene with 0.4 L, 6M HCL for 24 h to remove basic nitrogenous material, then refluxed with 40% NaOH for 2 h to remove benzonitrile. Extraction by *n*-hexane was followed by washing with water (three times), drying with MgSO<sub>4</sub>, and evaporation of the *n*-hexane. Fractionized distillation under reduced pressure is repeated until indene fractions with purities higher than 98% were reached. Gas chromatography in combination with mass spectroscopy (GC-MS) showed that the amount of polymerizable impurities was negligible (undecene concentration < 0.03%). From this, it

**Table I MA–Ind Emulsion Copolymerization Recipes of Reactions Performed to Achieve Optimum Concentrations of NPS and Ant CO-990,  $f_{o,MA} = 0.5$  and M/W = 0.1**

Ingredients	
MA (g)	3.8
Ind (g)	5.2
Water (g)	90
NPS (mmol/L)	10–25
Ant CO-990 (mmol/L)	2.5–12.5
Na <sub>2</sub> CO <sub>3</sub> (mmol/l)	10

was concluded that the indene could be used without further purification. The indene is stored under argon at 4°C.

### Emulsion Copolymerizations

The emulsion copolymerizations described in this article can be divided into two categories: (1) polymerizations to determine optimum concentrations of surfactant (Ant CO-990) and initiator (NPS), resulting in stable latices and reasonable polymerization rates, and (2) polymerizations to study composition drift.

Emulsion copolymerizations to determine optimum concentrations of surfactant and initiator were carried out in 100 mL reactors thermostated at 70°C and mixed with a magnetic stirrer. Since our main interest was obtaining reasonable polymerization rates, these reactions were followed by gravimetry only. For the MA–Ind copolymerization, high initiator concentrations were needed to give reasonable polymerization rates, resulting in unstable latices due to high electrolyte concentrations. The use of nonionic Ant CO-990 instead of SDS gave satisfying results. The recipes used to determine optimum concentrations for the emulsion copolymerizations are shown in Table I.

Emulsion polymerizations to study composition drift were performed in a 1.3 L stainless-steel reactor fitted with four baffles at 90° intervals and a six-bladed turbine impeller. The recipes for these emulsion copolymerizations, which were performed using the same overall monomer mole fraction of  $f_{o,MA} = 0.75$  and varying monomer-to-water ratios are given in Table II. The MA–Ind copolymerizations were performed under nitrogen at 70°C for 12 h. All reactions concerning composition drift were monitored by gravimetry, yielding conversion–time curves, and by GC, providing the overall monomer fractions as a function of time. The GC analyses were performed utilizing a Hewlett-Packard (HP) 5890A gas chromatograph, an HP 3393A integrator, an HP 7673A automatic sampler, and a capillary chromopack CP-sil 19CB column with a length of 25 m, an internal diameter of 0.53 mm, and a film thickness of 2 μm. An indication of the accuracy of data analyses was obtained by adding known amounts of *n*-butanol as internal standard to the GC samples in order to obtain extra conversion–time data. Combining both data gives the overall conversion of both monomers at each moment during the reaction.

### Determination of the Reactivity Ratios from Bulk Polymerizations

Bulk copolymerizations were carried out in 20 mL bottles thermostated at 70°C and mixed with a magnetic stirrer. The reaction mixture consisted of 20 g of monomer with different monomer mole fractions going from 10 to 90% MA and 0.1 g AIBN as initiator. The reactions were stopped at low conversion (< 3%) in order to prevent composition drift. The copolymer composition of the polymer formed was determined by <sup>1</sup>H-NMR. The resulting monomer feed fraction–copolymer composition data are shown in Table III.

**Table II MA–Ind Emulsion Copolymerization Recipes of Reactions Performed to Investigate the Effect of Monomer-to-Water Ratios on Compositional Drift,  $f_{o,MA} = 0.75$** 

Ingredients	M/W = 0.4	M/W = 0.3	M/W = 0.1
MA (g)	165.47	144.87	62.09
Ind (g)	74.41	64.46	27.83
Water (g)	600.1	700.3	898.8
NPS (mmol/L)	26.31	25.05	24.90
Ant CO-990 (mmol/L)	7.449	7.498	7.539
Na <sub>2</sub> CO <sub>3</sub> (mmol/L)	9.968	9.916	10.035

**Table III Low Conversion Bulk Polymerization Data**

Monomer Feed Fraction $f_{MA}$	Copolymer Composition $F_{MA,experimental}$	Copolymer Composition $F_{MA,theoretical}$
0.105	0.393	0.379
0.210	0.483	0.478
0.308	0.534	0.537
0.405	0.585	0.587
0.510	0.642	0.641
0.606	0.700	0.694
0.655	0.726	0.723
0.711	0.766	0.758
0.804	0.825	0.823
0.903	0.904	0.904

## RESULTS AND DISCUSSION

To achieve reasonable polymerization rates in MA-Ind emulsion copolymerization reactions, high initiator concentrations were needed (see Table I for standard recipes). Reactions performed with surfactant SDS, frequently used in emulsion polymerization, did not result in colloidally stable latices for any SDS concentration (going from 10 to 75 mmol/L). From this, it was concluded that the high electrolyte concentrations resulting from the high initiator and buffer concentrations were causing the coagulation. The use of the nonionic surfactant Ant CO-990 instead of SDS resulted in colloidally stable latices. The surfactant and initiator concentrations were optimized resulting in concentrations of 7.5 and 10 mmol/L, respectively.

Some typical conversion-time curves for the emulsion copolymerization of MA-Ind (recipes are listed in Table I) can be seen in Figure 2 for several initiator (NPS) concentrations. From Figure 2, it can be concluded that the overall polymerization rate increases with increasing NPS concentrations, as can be expected from emulsion polymerization theory. Experiments performed with increasing surfactant (Ant CO-990) concentrations showed a slight increase in polymerization rate. Particle-size analysis by dynamic light scattering (Malvern Autosizer IIc) showed that the particle size decreased with increasing initiator and surfactant concentrations. This behavior is typical of emulsion polymerization,<sup>26</sup> since by using more surfactant, more particle surface can be stabilized. Increasing the initiator concentration leads to higher radical concentrations in the beginning of the reaction and, therefore, more particles can be nucleated.

Comparison of gravimetry and GC results is

shown in Figure 3 for the MA-Ind reaction at a monomer-to-water ratio of 0.1 g/g (recipe: Table II). For the reaction shown in Figure 3, it can be concluded that the polymerization rate of Ind is higher than the polymerization rate of MA, resulting in a copolymer composition that is more Ind-rich in the beginning and more MA-rich toward the end of the polymerization as compared with the initial overall monomer mole fraction. The accuracy of the experimental results is illustrated by the good agreement when comparing the total conversion-time curves obtained from gravimetry with the data obtained from GC analysis using an internal standard, enabling the determination of not only monomer ratios but also conversion data of the separate monomers. Note that the internal standard was added afterward to samples taken from the reaction since, otherwise, monomer partitioning during re-

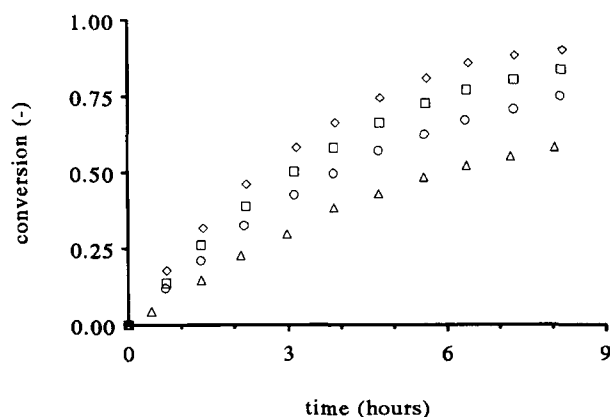


**Figure 2** Conversion-time curves typical of MA-Ind emulsion copolymerization for initiator (NPS) concentrations of ( $\Delta$ ) 10 mmol/L, ( $\circ$ ) 15 mmol/L, ( $\square$ ) 20 mmol/L, and ( $\diamond$ ) 25 mmol/L.

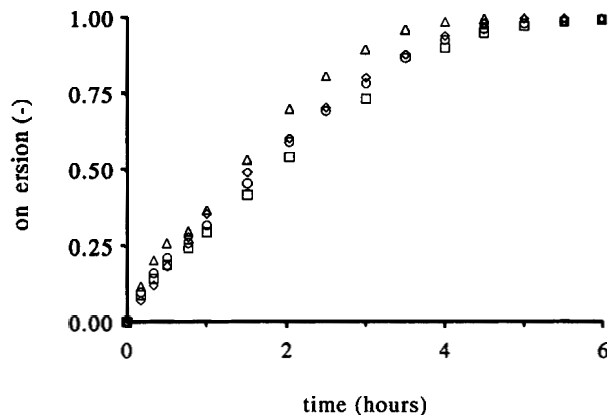


**Figure 3** Experimental conversion-time results for MA-Ind emulsion copolymerization at  $M/W = 0.1$  and  $f_{0MA} = 0.75$ . The total conversion curves are based on ( $\diamond$ ) gravimetry and ( $\circ$ ) GC data; the conversion-time curves of the separate monomers [( $\square$ ) MA; ( $\triangle$ ) Ind] are based on GC data only.

action would have been affected by the internal standard. All MA-Ind emulsion copolymerization experiments performed to study composition drift behavior were analyzed in the above manner.

### Reactivity Ratios

Predictions of the course of emulsion copolymerizations can be made by using a recently developed

method<sup>23</sup> that is very convenient since it only requires the reactivity ratios and the homosaturation values of the monomers in the aqueous and polymer phase to be known. Accurate reactivity ratios are needed to predict the course of copolymer composition in emulsion copolymerization as a function of conversion. For monomer combinations like MA-Ind that have not been extensively studied, low-conversion bulk polymerizations have to be performed to determine reliable reactivity ratios. The copolymer compositions resulting from the low-conversion bulk polymerizations were determined by  $^1\text{H-NMR}$ . Figure 4 depicts a typical example of a 400 MHz  $^1\text{H-NMR}$  spectrum of low-conversion bulk MA-Ind copolymers dissolved in  $\text{CDCl}_3$  at  $25^\circ\text{C}$ . The average copolymer composition (mole fraction MA:  $F_{MA}$ ) can be calculated with the following formula:

$$F_{MA} = \frac{2 \cdot B - 2 \cdot A}{2 \cdot B + A} \quad (2)$$

where  $A$  and  $B$  represent the total peak area of the aromatic (4 H of Ind) and aliphatic (4 H of Ind and 6 H of MA) protons, respectively. The reactivity values were determined by nonlinear optimization<sup>27</sup> of the monomer feed-copolymer composition data summarized in Table III. When calculating reactivity ratios with this nonlinear optimization method, errors in both the monomer feed composition (es-

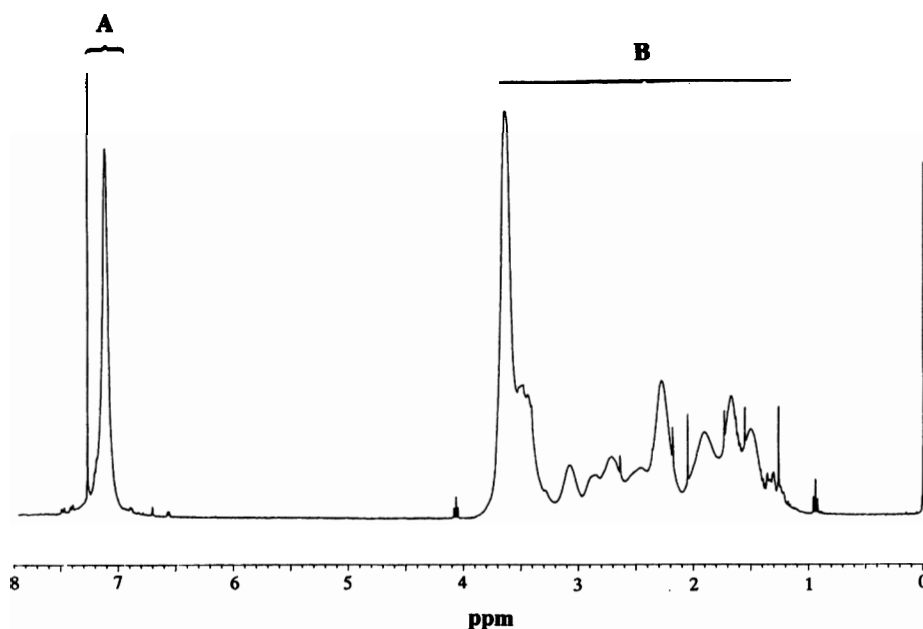


**Figure 4**  $^1\text{H-NMR}$  spectrum typical of an MA-Ind copolymer. A and B stand for the total peak areas in the aromatic and aliphatic regions, respectively.

timated to be 1%) and the copolymer composition (estimated to be 5%) are taken into account. This results in the following reactivity data:  $r_{MA} = 0.92 \pm 0.16$  and  $r_{Ind} = 0.086 \pm 0.025$ . When using these reactivity ratios, the monomer feed–copolymer composition relation can be described theoretically using the instantaneous copolymer equation [eq. (1)]. Comparing experimental results with the theoretical prediction of the instantaneous copolymer equation gives good agreement, as can be seen in Figure 5 and Table III. From the results, it can be concluded that reliable values for the reactivity ratios for MA–Ind have been obtained.

### Monomer Partitioning

For model calculations,<sup>23</sup> not only are reactivity ratios needed, but also the homomonomer saturation concentrations in the polymer and aqueous phase. These homomonomer saturation concentrations, better known as the water solubility and swellability of the separate monomers in the aqueous and polymer phases, were determined by monomer partitioning experiments using the ultracentrifuge method.<sup>21,22,23,28</sup>

Although the absolute concentrations of monomers in the particle phase strongly depend upon the homosaturation concentrations of the monomers in the polymer particle phase, it has been shown in the

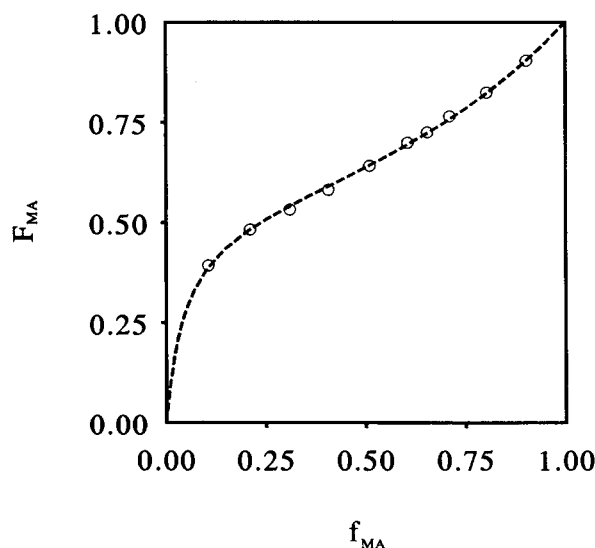


**Figure 5** Comparison of the monomer feed–polymer composition data (---) predicted with the instantaneous copolymer equation using the reactivity values of  $r_{MA} = 0.92$  and  $r_{Ind} = 0.086$  and (○) experimentally determined data from low conversion bulk polymerizations.

literature<sup>22,23,29</sup> that the monomer ratio within the polymer phase is independent of the maximum swellability of both monomers in the polymer phase, i.e., independent of the copolymer composition, at saturation swelling. Therefore, it can be concluded that changing copolymer composition as a function of conversion occurring at saturation swelling may affect the rate of polymerization (changing absolute concentrations) but certainly not the composition drift (constant monomer ratio within the particles).

At partial swelling, monomer partitioning between the aqueous and polymer phases depends upon the volume fraction of polymer, i.e., it depends on the maximum swellability in the polymer of the monomers. The change in maximum swellability as a function of copolymer composition has been shown to be negligible<sup>23,30,31</sup> for several monomer systems. Furthermore, the effects of possible changes in copolymer composition on monomer partitioning leading to different maximum swellabilities can be estimated using the following equations<sup>23</sup>:

$$\nu_p = 1 - \%satp(1 - \nu_{p,sat}) \quad (3b)$$

$$\ln\left(\frac{\%satp}{\%sata}\right) = \nu_{p,sat} - \nu_p \quad (3a)$$

where %satp, %sata,  $\nu_{p,sat}$ , and  $\nu_p$  represent the degree of saturation in the polymer and aqueous phases and the volume fraction of polymer at saturation and below saturation swelling, respectively. Using eqs. 3(a) and (b), the effects of changing monomer composition on the (maximum) volume fractions of a polymer can be taken into account in model predictions,<sup>23</sup> whereas the effect of changing copolymer composition can be estimated assuming maximum swellabilities of a monomer mixture (50% MA–50% Ind; normal swellability of 5 mol/L) in the homopolymer–Ind of 4 mol/L ( $\nu_{p,sat} = 0.53$ ) and in the homopolymer–MA of 6 mol/L ( $\nu_{p,sat} = 0.36$ ). From Figure 6, where the degree of saturation in the polymer phase is depicted as a function of the degree of saturation in the aqueous phase, it can be concluded directly that the effects of changing copolymer composition going from pInd to pMA has a relatively small influence on monomer partitioning. In practical situations, these effects will even be smaller since the change in copolymer composition is less drastic than that presented in Figure 6.

Based on the above discussion, all effects of changing maximum swellabilities of the monomer in the polymer phase as a result of changing copolymer composition are neglected for saturation and

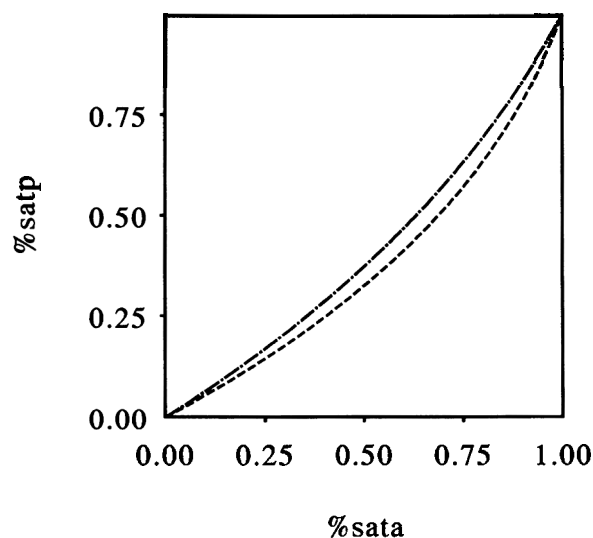


**Figure 6** Model predictions of the degree of saturation in the polymer phase, %satp, as a function of the degree of saturation in the aqueous phase, %sata, using eqs. 3 (a) and (b) with saturation volume fractions of polymer  $\nu_{p,sat}$  of (---) 0.53 and (-·-·-) 0.39.

partial swelling. All model predictions are carried out using one set of homosaturation concentrations of MA and Ind that have been determined by monomer partitioning experiments in a 50% MA–50% Ind seed.

Since the water solubility of both monomers in the aqueous phase has a large effect<sup>23</sup> on monomer partitioning in both saturation and partial swelling, accurate homosaturation concentrations of the monomers in the aqueous phase at reaction temperature are needed. The maximum temperature under which centrifugation can be performed is 45°C. Therefore, a different approach had to be used to obtain the water solubility of MA at higher temperatures. For this reason, the density of thermostated MA–water solutions with increasing MA to water content (below saturation) was measured at the desired temperature, resulting in a straight line of density values as a function of monomer-to-water content. An MA–water mixture far above saturation was allowed to undergo phase separation. From the saturated aqueous phase, a sample was taken for densimetry, resulting in the density of the saturated aqueous phase. Extrapolation of the straight density–monomer-to-water ratio line then resulted in the monomer-to-water ratio at saturation, i.e., in the water solubility. The maximum water solubility of MA at 70°C as determined by densimetry is listed in Table IV together with other monomer partitioning results for the system MA–Ind.<sup>23</sup>

### Composition Drift in Emulsion Copolymerization of MA–Ind

The monomer mole fraction in the polymer phase is determined by monomer partitioning. Changing the monomer-to-water ratio or the polymer volume in a monomer–water–polymer mixture will lead to different monomer mole fractions in the polymer phase.<sup>23</sup> This effect will be especially large if one of the monomers has a relatively high but still limited water solubility, as, for instance, MA.

In this article, monomer  $i$  is assumed to be the more water-soluble one, resulting in two extreme values for the monomer mole fraction in the polymer phase, i.e., the maximum value  $f_{pi,max}$  that is reached if all monomer is located in the polymer phase and the minimum value  $f_{pi,min}$  that is reached if all monomer is dissolved in the aqueous phase.

The maximum value of the monomer mole fraction of monomer  $i$  in the polymer phase,  $f_{pi,max}$ , is reached at saturation swelling when the amount of monomers in the aqueous phase is negligible as compared with the total amount of monomers (large monomer droplet and polymer particle phases as compared with aqueous phase) or if the water-phase concentrations are too low to significantly affect the monomer amounts within the monomer droplet and polymer particle phases. In these cases, the monomer mole fraction of monomer  $i$  in the polymer phase equals the overall mole fraction of monomer  $i$ , i.e.,  $f_{pi,max} = f_{oi}$ . The minimum value for the mole fraction of monomer  $i$  in the polymer particle phase,  $f_{pi,min}$ , is reached when all monomer is located in the aqueous phase. In this case, the mole fraction of monomer  $i$  in the aqueous phase equals the overall monomer mole fraction of this monomer, i.e.,  $f_{ai} = f_{oi}$ . From this mole fraction of monomer  $i$  in the aqueous phase, the minimal mole fraction of monomer  $i$  within the polymer phase,  $f_{pi,min}$ , can be determined with eq. (4)<sup>22,23</sup> if the ratio of the water

**Table IV** Monomer Partitioning Data and Reactivity Ratios

	MA	Ind
Reactivity ratios	0.92 ± 0.16	0.086 ± 0.025
Water solubility (mol/L)	0.53 <sup>a</sup>	0.0028 <sup>b</sup>
Swellability (mol/L)	7.1 <sup>b</sup>	2.9 <sup>b</sup>

<sup>a</sup> Determined by densimetry at 70°C.

<sup>b</sup> Determined by the ultracentrifugation method at 20°C.



solubilities of monomer  $j$  over monomer  $i$ , i.e., if  $\alpha = [M_j]_{a,sat}(h)/[M_i]_{a,sat}(h)$ , is known:

$$f_{ai} = \frac{f_{pi}}{f_{pi} \cdot (1 - \alpha) + \alpha} \quad (4)$$

The value of  $f_{pi,min}$  strongly depends upon the  $\alpha$ -value,<sup>23</sup> leading to larger differences between  $f_{pi,max}$  and  $f_{pi,min}$  for smaller  $\alpha$ -values. This  $f_{pi,min}$  can be reached only if at least one of the monomers has a relatively high water solubility and if the monomer-to-water ratio is low and if the amount of polymer phase is too small to affect monomer partitioning. It is important to realize that although the minimum monomer mole fraction in the polymer only depends on the ratio of the water solubilities,  $\alpha$ , the absolute water solubility values are determining the monomer-to-water ratio needed to obtain this minimum monomer mole fraction in the polymer phase.

Depending on recipe conditions, like monomer-to-water ratio ( $M/W$ ) and polymer volumes ( $V_{po}$ ), the value for the mole fraction of monomer  $i$  in the polymer phase will vary between  $f_{pi,max}$  and  $f_{pi,min}$ .

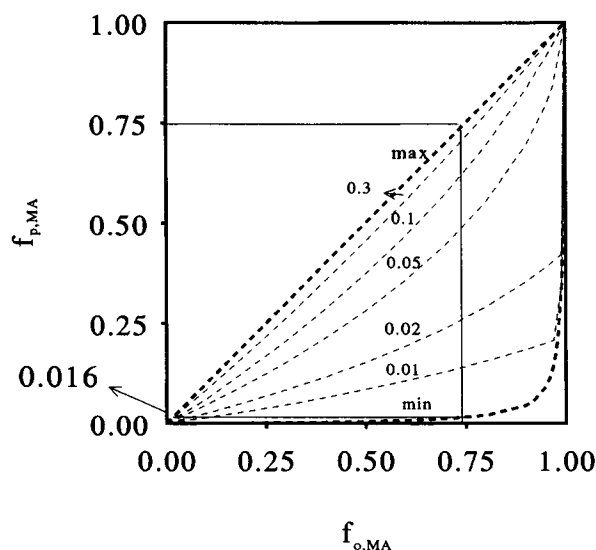


**Figure 7** Monomer mole fractions in the polymer phase,  $f_{p,MA}$ , as a function of the overall monomer mole fraction for the monomer system MA-Ind: minimum (min), maximum (max), and monomer-to-water ratio dependent ( $M/W = 0.01, 0.02, 0.05, 0.1, 0.3$ ).

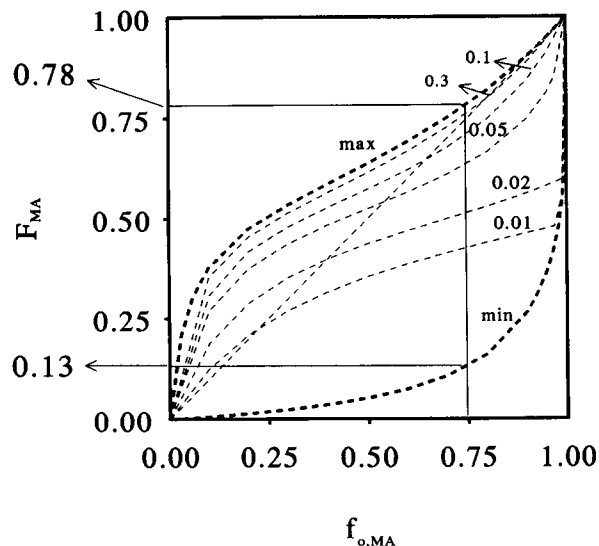


**Figure 8** Monomer mole fractions in the copolymer,  $F_{MA}$ , (resulting from  $f_{p,MA}$  data presented in Fig. 7) as a function of the overall monomer mole fraction,  $f_{o,MA}$ , for the monomer system MA-Ind: instantaneous copolymer compositions resulting from the minimum (min), maximum (max), and monomer-to-water ratio-dependent ( $M/W = 0.01, 0.02, 0.05, 0.1, 0.3$ ). The diagonal line represents the conditions needed to obtain azeotropic conditions, i.e., overall monomer mole fraction is equal to instantaneous copolymer composition.

In Figure 7, the maximum and minimum values for the monomer mole fraction in the polymer phase as a function of the overall monomer mole fraction are given for the monomer system MA-Ind in which  $\alpha = 0.0053$ . Due to the large difference in water solubility of MA as compared with Ind, expressed in the low  $\alpha$ -value, the monomer mole fraction in the polymer phase is strongly affected by changing monomer-to-water ratios. This effect of  $M/W$  on the mole fraction of monomer  $i$  in the polymer phase in the absence of polymer is also clearly shown in this Figure 7.

The copolymer composition resulting from the maximum and minimum values for the monomer mole fraction in the polymer phase can be calculated with eq. (1) using the reactivity values  $r_{MA} = 0.92$  and  $r_{Ind} = 0.086$ . These copolymer compositions, which are typical of each monomer system with given  $\alpha$ -value and reactivity ratios, are depicted in Figure 8 together with the diagonal line representing azeotropic conditions, i.e., overall monomer mole fraction equal to instantaneous copolymer composition. From Figure 8, one can see directly the minimum and maximum instantaneous copolymer compositions obtainable when starting from a given

overall monomer mole fraction in an emulsion copolymerization of MA–Ind. The strong effect of varying monomer-to-water ratios on the instantaneous copolymer composition is also depicted in Figure 8. To illustrate the minimum and maximum mole fractions of monomer  $i$  and the resulting instantaneous copolymer compositions, an example is shown in Figures 7 and 8 for an overall monomer mole fraction of  $f_{oMA} = 0.75$ . For low monomer-to-water ratios without polymer (almost all monomers located in the aqueous phase), one can see that the minimum monomer mole fraction in the polymer phase is reached,  $f_{pMA,min} = 0.016$ , (Fig. 7), resulting in a copolymer composition of  $F_{MA} = 0.13$  (Fig. 8), whereas at high monomer-to-water ratios, the maximum monomer mole fraction is reached,  $f_{pMA,max} = 0.75$  (Fig. 7), resulting in a copolymer composition of  $F_{MA} = 0.78$  (Fig. 8).

We have already seen that azeotropic conditions occur only if the instantaneous copolymer composition equals the overall monomer mole fraction. Knowing this, one can see in Figure 8 that the intersection of the lines representing minimum, maximum, and M/W-dependent values for the instantaneous copolymer composition with the diagonal gives the conditions needed to obtain azeotropic conditions, i.e., instantaneous copolymer composition equals overall monomer mole fraction. Calculation shows that these azeotropic conditions can be found for  $f_{oMA}$  values between 0 and 0.91 at low conversion. However, the aim of this work was to achieve minimum composition drift over a wider range of conversion and is not restricted to low con-

version. Therefore, the overall monomer mole fraction needed for minimum composition drift over the entire range of conversion may deviate slightly from the conditions represented by the intersections of the diagonal and the copolymer compositions shown in Figure 8.

Experimental results of emulsion copolymerization composition as a function of conversion have been compared with the model presented by Noël et al.<sup>23</sup> for MA–Ind systems. The large effect of different monomer-to-water ratios on the system MA–Ind, with a relatively water-soluble monomer like MA, can be seen in Figure 9, where theory and experiment are compared, resulting in very good agreement (initial reaction recipes are shown in Table II). In case of MA–Ind emulsion copolymerizations, more of the more water-soluble MA will be buffered in the aqueous phase at lower monomer-to-water ratios as compared with higher monomer-to-water ratios. As can be seen in Figure 9, minimum or even reversed composition drift can be achieved by simply changing the monomer-to-water ratio in a batch emulsion copolymerization of MA–Ind.

What exactly happens in the emulsion copolymerizations of MA–Ind at an overall monomer ratio of MA with varying monomer to water ratios is depicted more clearly in Figure 10, where theoretical and experimental (calculated with monomer partitioning equations<sup>22,23</sup>) mole fractions of MA in the polymer phase are compared. In case of MA–Ind emulsion copolymerizations, a larger part of the more water-soluble MA will be buffered in the aqueous phase at lower monomer-to-water ratios,

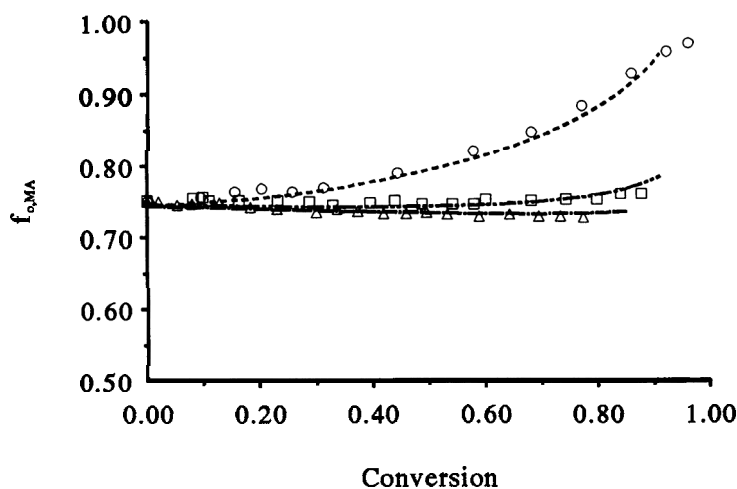


**Figure 9** Comparison of predicted and experimentally determined overall monomer mole fractions for the monomer system MA–Ind, with initial overall monomer mole fraction of  $f_{oMA} = 0.75$  and different monomer-to-water ratios (M/W) of 0.1 [(- - -) prediction; (○) experiment] 0.3 [(- · - · -) prediction; (□) experiment], and 0.4 [(- · - · -) prediction].

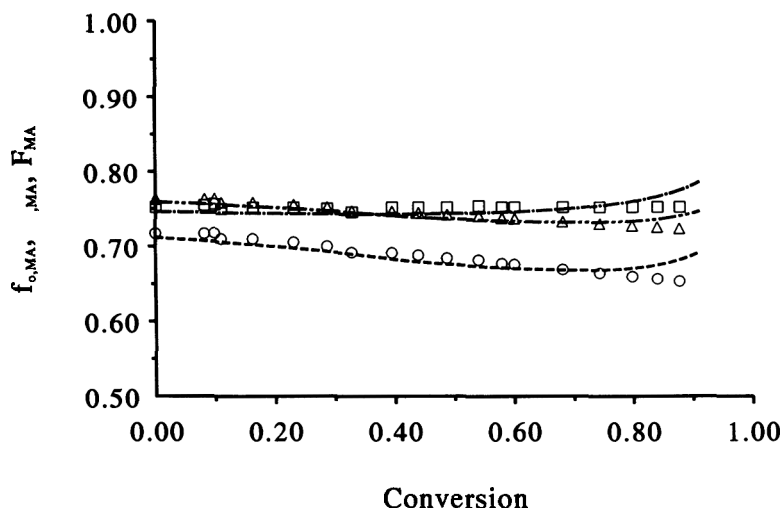


**Figure 10** Comparison of model prediction (lines) with experimental results (symbols) of the mole fraction of MA in the polymer phase as a function of conversion, with an initial overall monomer mole fraction of  $f_{oMA} = 0.75$  and different monomer-to-water ratios (M/W) of (---;  $\circ$ ) 0.1, (-·-·-·;  $\Delta$ ) 0.3, and (-·-·-·;  $\square$ ) 0.4.

resulting in lower mole fractions of MA in the polymer phase at the beginning of the reaction. Composition drift at low M/W ratios (Fig. 10,  $f_{oMA} = 0.75$ , M/W = 0.1) shifts from instantaneous copolymer compositions with higher Ind contents than the initial overall feed in the beginning of the reaction, to instantaneous copolymer compositions with higher MA contents than the initial overall feed at the end of the reaction. At higher monomer-to-water ratios (Fig. 10,  $f_{oMA} = 0.75$ , M/W = 0.4), less MA is buffered in the aqueous phase, leading to composition drift shifting from higher monomer mole fractions of MA in the polymer phase in the beginning of the reaction (higher MA content in instantaneous copolymer than in the initial overall feed) to lower monomer mole fractions of MA in the end of the reaction (higher Ind content in the instantaneous copolymer than in the initial overall feed). From Figures 9 and 10, we can conclude that composition drift can indeed be minimized by varying the monomer-to-water ratio in MA-Ind emulsion copolymerization. For overall monomer mole fractions of MA of  $f_{oMA} = 0.75$  minimum composition drift is achieved for monomer-to-water ratios of M/W = 0.3.

The course of emulsion copolymerization at minimum composition drift is shown in more detail in Figure 11, where model predictions<sup>23</sup> of  $f_{pMA}$  and  $f_{oMA}$  and resulting from this the mole fraction of MA in the copolymer ( $F_{MA}$ ) are compared with experiments ( $f_{pMA}$  and  $F_{MA}$  are calculated from  $f_{oMA}$  and overall conversion using monomer partitioning

relationships<sup>22,23</sup> and the instantaneous copolymer equation). As could be expected at minimum composition drift conditions, all three compositions,  $f_{pMA}$ ,  $f_{oMA}$ , and  $F_{MA}$  are more or less constant as a function of conversion. Another important result of Figure 11 is that the prerequisite for minimum composition drift, i.e.,  $f_{oMA}$  equal to  $F_{MA}$  (see Fig. 8), is apparently approximated during the reaction. In Figures 7 and 8, it is illustrated that by simply changing initial reaction conditions like the monomer-to-water ratio one can reach minimum composition drift, if desired. In case the occurrence of composition drift is desired, one can change the monomer-to-water ratio in such a way as to achieve composition drift in the desired direction and to the desired extent.

As can be seen in Figure 8, minimum composition drift conditions can also be achieved for other overall monomer mole fractions. From Noël et al.<sup>22,23</sup> and from the good agreement between predictions and experimental results shown in Figure 9, it can be concluded that the model<sup>23</sup> used to predict the course of emulsion copolymerization can provide good simulations of copolymer composition in emulsion copolymerization, even under conditions as critical as those leading to minimum composition drift. Therefore, the presented model can be used, in combination with the experimentally determined homonomer saturation values and reactivity ratios, to predict the monomer-to-water ratio needed to achieve minimum composition drift for several overall monomer mole fractions for the monomer

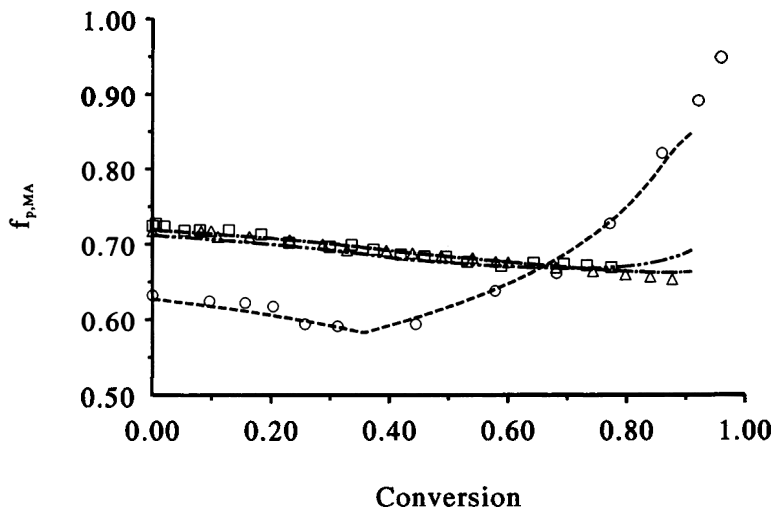


**Figure 11** Comparison of model predictions (lines) and experimental results (symbols) of (---;  $\circ$ )  $f_{p,MA}$ , (-·-·-;  $\square$ )  $f_{o,MA}$ , and (-·-·-·-;  $\triangle$ )  $F_{MA}$  as a function of conversion for the emulsion copolymerization of MA-Ind with  $M/W = 0.3$  and  $f_{o,MA} = 0.75$ , resulting in minimum composition drift.

system MA-Ind. The monomer-to-water ratios needed to obtain this minimum composition drift at a given overall monomer mole fractions in MA-Ind emulsion copolymerization are shown in Figure 12. From these predicted results, we can conclude that minimum composition drift indeed can be achieved for other overall monomer mole fractions as well. Note, however, that realistic monomer-to-water ratios for batch emulsion copolymerizations normally are between  $0.1 < M/W < 2$ . Note also that the assumption of negligible polymerization in the aqueous phase may not longer be valid at low mono-

mer-to-water ratios. In this case, a considerable percentage of the polymerization might occur in the aqueous phase. One way to avoid this from happening might be the use of an oil-soluble initiator in combination with an aqueous-phase free-radical scavenger or retarder as an alternative of the water-soluble initiator NPS.

It is important to realize that minimizing composition drift in MA-Ind reactions is possible due to the moderate difference in reactivity values of the monomers (a factor of 10) combined with a large difference in homonomer saturation concentra-

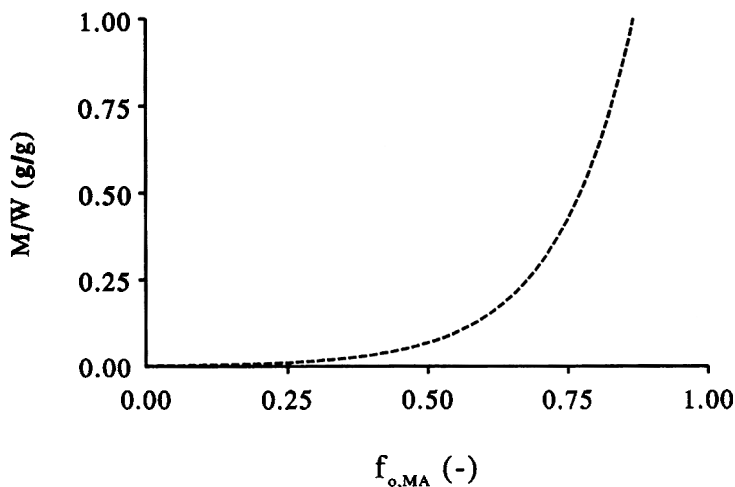


**Figure 12** Model prediction of the monomer-to-water ratio as a function of the overall monomer mole fraction of MA needed to achieve minimum composition drift.

tions (factor  $\alpha = 0.05$ ). In this case, the water phase can buffer a sufficient amount of the more reactive monomer to minimize composition drift.

The intrinsic possibility of achieving minimum composition drift in batch emulsion copolymerization for other monomer systems can be determined directly when the water solubilities of the monomers ( $\alpha$ ) and the reactivity values are known for a given monomer system. The maximum monomer mole fraction in the polymer phase always equals the overall monomer mole fraction. If the reactivity ratios of the chosen monomer systems are known, the copolymer composition resulting from the maximum monomer mole fraction in the polymer phase can be calculated with eq. (1). It was shown that the minimum monomer mole fraction in the polymer phase is reached when the monomer mole fraction in the aqueous phase was equal to the overall monomer mole fraction. From this monomer mole fraction in the aqueous phase, the minimum monomer mole fraction in the polymer phase can be calculated directly with eq. (4) if the ratio of the water solubilities of the monomers, the  $\alpha$ -value, is known for the chosen monomer system. The copolymer composition resulting from this minimum monomer mole fraction in the polymer phase again can be calculated using eq. (1) if the reactivity ratios are known. If the copolymer compositions resulting from the minimum and maximum monomer mole fractions in the polymer phase are higher and lower, respectively, than the overall monomer mole fraction, the prerequisite for minimum composition drift, i.e., equal overall monomer mole fraction to instantaneous copolymer composition, can be achieved for the selected overall monomer mole fraction. The procedure described here can be used for any monomer system at every desired overall monomer mole fraction, giving similar results as shown in Figures 7 and 8 for MA-Ind emulsion copolymerizations.

## CONCLUSIONS

Reactivity ratios for MA-Ind have been determined by low conversion bulk polymerization, resulting in  $r_{MA} = 0.92 \pm 0.16$  and  $r_{Ind} = 0.086 \pm 0.025$  (70°C).

Theory predicts that for monomer systems in which the water solubility of the monomers is sufficiently far apart (low  $\alpha$ -values) minimum composition drift can be achieved by changing the initial monomer-to-water ratio in a batch emulsion copolymerization in which the more reactive monomer is also the more water-soluble one. Experimental verification of this theoretical prediction has shown

that minimum composition drift could be achieved for the monomer system MA-Ind were MA is the more reactive and more water-soluble monomer. Model predictions show that composition drift can be minimized for MA-Ind emulsion copolymerization for a wide range of overall monomer mole fractions, simply by choosing different initial monomer-to-water ratios.

It should be noted that the approach presented in this article always gives information about the span of control of the composition drift even in those cases where minimum composition drift cannot be achieved.

## REFERENCES

1. K. Chujo, Y. Harada, S. Tokuhara, and K. Tanaka, *J. Polym. Sci. Part C*, **27**, 321 (1969).
2. J. Šnupárek, *Angew. Makromol. Chem.*, **25**, 113 (1972).
3. R. A. Wessling and D. S. Gibbs, *J. Macromol. Sci. Chem.*, **A-7**, 647 (1973).
4. J. Šnupárek and F. Krška, *J. Appl. Polym. Sci.*, **20**, 1753 (1976).
5. J. Šnupárek and F. Krška, *J. Appl. Polym. Sci.*, **21**, 2253 (1977).
6. J. Šnupárek and K. Kašpar, *J. Appl. Polym. Sci.*, **26**, 4081 (1981).
7. M. S. El-Aasser, T. Makgawinita, and J. W. Vanderhoff, *J. Polym. Sci. Polym. Chem. Ed.*, **21**, 2363 (1983).
8. S. C. Misra, C. Pichot, M. S. El-Aasser, and J. W. Vanderhoff, *J. Polym. Sci. Polym. Chem. Ed.*, **21**, 2383 (1983).
9. T. Makgawinita, M. S. El-Aasser, A. Klein, and J. W. Vanderhoff, *J. Dispersion Sci. Technol.*, **5**, 301 (1984).
10. G. Arzamendi and J. M. Asua, *J. Appl. Polym. Sci.*, **38**, 2019 (1989).
11. G. Arzamendi and J. M. Asua, *Makromol. Chem. Macromol. Symp.*, **35/36**, 249 (1990).
12. G. Arzamendi and J. M. Asua, *Ind. Eng. Chem. Res.*, **30**, 1342 (1991).
13. G. H. J. van Doremaele, H. A. S. Schoonbrood, J. Kurja, and A. L. German, *J. Appl. Polym. Sci.*, **45**, 957 (1992).
14. G. Arzamendi, J. C. de la Cal, and J. M. Asua, *Angew. Makromol. Chem.*, **194**, 47 (1992).
15. G. H. J. van Doremaele, PhD Thesis, Eindhoven University of Technology, Eindhoven, The Netherlands, 1990.
16. M. Morton, S. Kaizermann, and M. W. Altier, *J. Colloid Sci.*, **9**, 300 (1954).
17. J. L. Gardon, *J. Polym. Sci. Polym. Chem. Ed.*, **6**, 2859 (1968).
18. J. Ugelstad, P. C. Mork, H. R. Mfutakamba, E. So-

- leimany, I. Nordhuus, R. Schmid, A. Berge, T. Ellingsen, O. Aune, and K. Nustad, in *Science and Technology of Polymer Colloids*, Vol. 1, G. W. Poehlein, R. H. Ottewill, and J. W. Goodwin, Eds., NATO ASI Ser., 1983.
19. J. Guillot, *Acta Polym.*, **32**, 593 (1981).
20. C. M. Tseng, M. S. El-Aasser, and J. W. Vanderhoff, *Org. Coat. Plast. Chem.*, **45**, 373 (1981).
21. I. A. Maxwell, J. Kurja, H. J. van Doremale, and A. L. German, *Makromol. Chem.*, **193**, 2065 (1992).
22. L. F. J. Noël, I. A. Maxwell, and A. L. German, *Macromolecules*, **26**, 2911 (1993).
23. L. F. J. Noël, I. A. Maxwell, J. M. A. M. van Zon, and A. L. German, to appear.
24. T. Alfrey and G. Goldfinger, *J. Chem. Phys.*, **12**, 205 (1944).
25. F. R. Mayo and F. M. Lewis, *J. Am. Chem. Soc.*, **66**, 1594 (1944).
26. R. M. Fitch and C. H. Tsai, *Polymer Colloids*, Plenum, New York, 1971.
27. M. Dube, A. Sanayei, A. Penlidis, K. F. O'Driscoll, and P. M. Reilly, *J. Polym. Sci. Polym. Chem.*, **29**, 703 (1991).
28. G. H. J. van Doremale, F. H. J. M. Geerts, H. A. S. Schoonbrood, J. Kurja, and A. L. German, *Polymer*, **33**, 1914 (1992).
29. A. M. Aerdt, M. M. W. A. Boei, and A. L. German, *Polymer*, **34**, 574 (1993).
30. G. H. J. van Doremale, F. H. J. M. Geerts, H. A. S. Schoonbrood, J. Kurja, and A. L. German, *Polymer*, **33**, 1914 (1992).
31. M. Nomura, K. Yamamoto, I. Horie, and K. Fujita, *J. Appl. Polym. Sci.*, **27**, 2483 (1982).

Received July 12, 1993

Accepted September 15, 1993